

## Zn-substitution effects on the optical conductivity in $\text{YBa}_2\text{Cu}_3\text{O}_{7-\delta}$ crystals: Strong pair breaking and reduction of in-plane anisotropy

N. L. Wang, S. Tajima, A. I. Rykov, and K. Tomimoto

*Superconductivity Research Laboratory, ISTEK, Shinonome 1-10-13, Koto-ku, Tokyo, 135 Japan*

(Received 24 November 1997)

Zn substitution effects on the  $a$ -,  $b$ -, and  $c$ -axis optical conductivity spectra have been investigated for optimally annealed  $\text{YBa}_2\text{Cu}_3\text{O}_{7-\delta}$  crystals. It was revealed that a very small amount of Zn seriously affects the low-energy charge dynamics in both normal and superconducting states. In addition to the increase of scattering rates, Zn substitution introduces additional features in the conductivity spectra and reduces the in-plane anisotropy by suppressing the plasma frequency in the  $b$  direction in the normal state. In the superconducting state, a very strong anisotropic pair-breaking effect was found. [S0163-1829(98)50318-9]

Zn substitution for Cu in high- $T_c$  superconductors has attracted much attention. A small amount of Zn not only reduces significantly the superconducting transition temperature  $T_c$  but also introduces substantial residual density of state as seen from the NMR (Ref. 1) and specific heat measurements.<sup>2</sup> Microwave surface impedance measurement in  $\text{YBa}_2\text{Cu}_3\text{O}_{7-\delta}$  (YBCO) crystals showed that only 0.15% Zn substitution for Cu alters the linear temperature dependence of the  $ab$ -plane penetration depth and 0.31% Zn changes it to a  $T^2$  dependence.<sup>3</sup> The muon-spin-relaxation ( $\mu\text{SR}$ ) measurement on Zn-doped YBCO polycrystalline samples also revealed very fast initial suppression of superfluid density.<sup>4</sup> These measurements were explained as the effect of impurity scattering in the unitary limit for a  $d$ -wave superconductor.

Optical spectroscopy is an important technique in probing the electronic state of a superconductor. Its advantage is that it can provide the information about both the normal carriers and the superconducting condensate, while the  $\mu\text{SR}$  measurement detects only the latter. Owing to the great improvement of the crystal growth technique, the detwinned YBCO single crystals with sufficiently large size have become available, which enables us to perform polarized optical measurements along all three crystallographic axes. In this paper, we report polarized optical spectra on pure and Zn-substituted single crystals in both normal and superconducting states. We show that a little bit of Zn has very strong but noticeably different effects on optical response in the three directions. The absolute values of the diagonal components of penetration depth tensor were estimated for these crystals. It has been revealed that the Zn substitution leads to very strong but anisotropic suppression of the condensate density along the three crystallographic axes.

High quality large single crystals of  $\text{YBa}_2(\text{Cu}_{1-x}\text{Zn}_x)_3\text{O}_{7-\delta}$  were prepared by a pulling technique and detwinned as described previously.<sup>5</sup> Zn concentration  $x$  in crystal was determined by inductively coupled plasma (ICP) spectrometry. All crystals were annealed at 500 °C in oxygen for two weeks, resulting in optimal oxygen content. The superconducting transition temperature, determined by both SQUID magnetization and resistivity, is 93 K for the pure sample, 85 K for  $x=0.4\%$ , 81 K for  $x=0.6\%$ ,

and 73 K for  $x=1.3\%$ . Prior to the optical measurements, the sample surfaces were polished by using  $\text{Al}_2\text{O}_3$  powder. The reflectivity measurements were performed in a fast scan Fourier transform spectrometer for  $\omega=50\text{--}9000\text{ cm}^{-1}$  and a grating type spectrometer for  $\omega=4000\text{--}30000\text{ cm}^{-1}$  at temperatures 8–295 K. The optical conductivity spectra were obtained from the reflectivity curves through the Kramers-Kronig transformation. For the low-frequency extrapolation, we use the Hagen-Rubens relation for reflectivity in the normal state and the two-fluid model in the superconducting state. For the high-frequency extrapolation, we connect our reflectivity curves to the earlier data by Tajima *et al.*<sup>6</sup>

The room temperature reflectivity spectra for Zn-free and Zn-substituted samples are shown in Fig. 1. The measurements for  $\mathbf{E}\parallel a$  and  $\mathbf{E}\parallel b$  were performed on the same sample, while the  $c$ -axis spectrum was measured on separate samples. The spectra of the Zn-free samples for all polarizations are in good agreement with the previous report.<sup>7</sup> The effects of Zn substitution on the spectra are found to be dependent on the polarization. In the  $c$ -axis spectrum, there is no clear effect of Zn substitution in the midinfrared and higher frequency ranges. In the main panel only one curve for  $\mathbf{E}\parallel c$  is shown because no distinct difference can be seen in this wide frequency range scale. For  $\mathbf{E}\parallel a$ , the derivative of reflectivity,  $dR/d\omega$ , seems to change. The two curves for the Zn-free and the Zn-substituted samples cross around  $5000\text{ cm}^{-1}$ . This suggests an increase of the Drude damping in this direction. A more striking Zn-substitution effect is observed in the spectrum for  $\mathbf{E}\parallel b$ . Namely, the reflectivity is suppressed over a wide frequency range up to the reflectivity minimum. This spectral change cannot be explained only by an increase of damping but requires a decrease of plasma frequency. The inset shows the reflectivity spectra in the far-infrared region. It is clearly demonstrated that Zn substitution affects the optical response in all three directions both in the normal and superconducting states. While in the Zn-free sample the low-frequency reflectivities become very close to unity at 8 K, reflecting an opening of a superconducting gap, they are appreciably lower in the Zn-substituted samples in all three directions, indicating some absorption in such frequencies. This absorption is attributed to the unpaired carriers which remain in the ground state. This can be seen more clearly from the conductivity spectra.

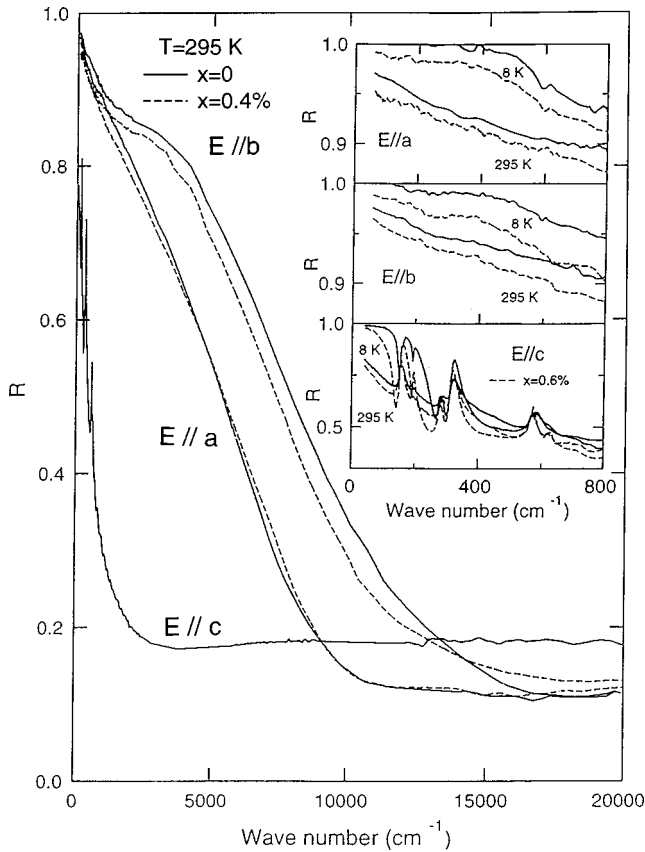


FIG. 1. The polarized reflectivity spectra for Zn-free and Zn-doped samples over a wide frequency range at room temperature. The inset shows the reflectivity spectra in the far-infrared region at 295 and 10 K.

The real part of conductivity spectra for pure and Zn-substituted crystals with  $\mathbf{E}\parallel a$ ,  $\mathbf{E}\parallel b$ , and  $\mathbf{E}\parallel c$  are shown in Fig. 2. In the normal state, the far-infrared conductivities in all three directions increase with decreasing temperature, which can be understood as a result of decrease of the Drude damping. A remarkable feature in the  $a$ -axis spectrum for the Zn-substituted sample is that the conductivity is substantially suppressed below  $120\text{ cm}^{-1}$ , giving rise to a peak in the spectrum. With decreasing temperature, the peak tends to be immersed in a steeply increasing free-electron conductivity without showing any appreciable shift in frequency. Similar peak structures have been observed in many cuprate superconductors and been attributed to carrier localization.<sup>8</sup> However, no sign of localization is observed in the dc resistivity of the Zn-substituted sample which is almost  $T$ -linear dependent with an additional residual resistivity due to the impurity scattering. We note that, despite the existence of the peak, the  $T$  dependence of the low- $\omega$  optical conductivity is consistent with this metallic dc resistivity behavior. The nature of such a peak remains to be elucidated. For  $\mathbf{E}\parallel b$ , although Zn also strongly affects the low-frequency conductivity, leading to a substantial reduction of conductivity at zero frequency, no clear peak is observed around  $120\text{ cm}^{-1}$ . Instead, a broad bump near  $1000\text{ cm}^{-1}$  becomes pronounced in the Zn-substituted sample. This bump was reported earlier and suggested to be associated with the disordered chains.<sup>9,10</sup> The observation indicates that the Zn substitution affects not only the  $\text{CuO}_2$  plane conductivity but also the chain conduction.

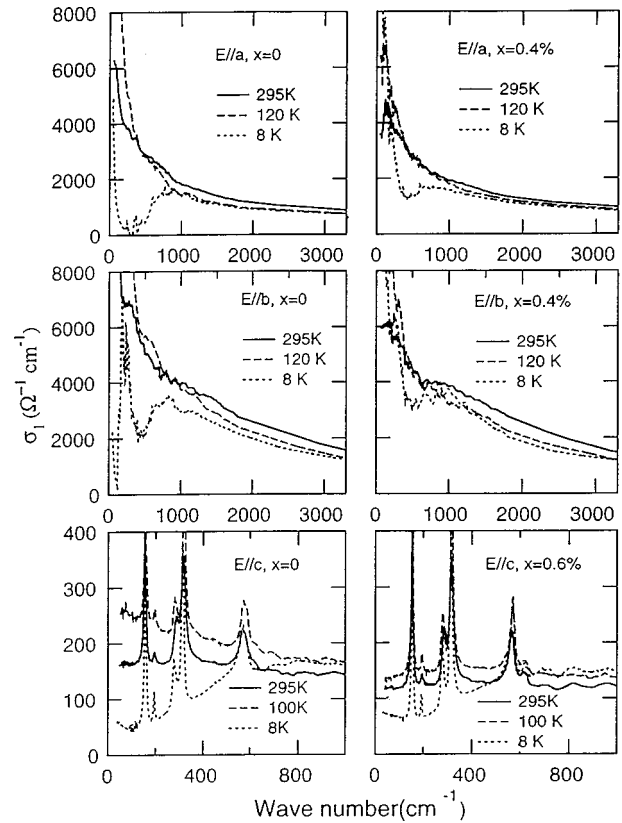


FIG. 2. Frequency-dependent conductivity spectra for Zn-free and Zn-doped crystals at different temperatures with  $\mathbf{E}\parallel a$ ,  $\mathbf{E}\parallel b$ , and  $\mathbf{E}\parallel c$ .

Because the crystals were annealed in the same condition, it is unlikely that the oxygen content in the Zn-substituted crystal is smaller than in the pure crystal. This was further supported by the fact that the Zn effect on the  $a$ -axis plasma frequency, estimated from the spectral weight up to  $10\,000\text{ cm}^{-1}$ , is very small, as we shall see later. The experimental observation can be explained by assuming that a small part of Zn occupies the Cu sites in the chains. Another possibility is that the  $\text{CuO}_2$  planes and  $\text{CuO}$  chains are strongly coupled. The Zn impurities in the  $\text{CuO}_2$  planes distort the local structure which affects the ordering of the  $\text{CuO}$  chains through the apical oxygen. Owing to the one-dimensional nature of the chains, such distortion or some Zn occupations on the chains may have a dramatic effect.

There are two possible ways to analyze the conductivity spectrum: one-component or two-component approaches.<sup>11</sup> In the present case there is no unambiguous way to decompose the conductivity spectrum into free-carrier and bound-carrier components because the spectra are  $T$  dependent over a wide frequency range and there also remains appreciable spectral weight in the far-infrared region even at the lowest temperature (8 K). Therefore, we analyzed the in-plane conductivity spectra by the extended Drude model. A comparison of the  $\omega$ -dependent scattering rates for  $\mathbf{E}\parallel a$  and  $\mathbf{E}\parallel b$  is shown in Fig. 3 for Zn-doped and Zn-free crystals at room temperature and 120 K. As well expected, the scattering rate or damping increases with Zn substitution, which must be responsible for the reduction of reflectivity and conductivity at low frequencies. The  $a$ -axis scattering rate changes almost linearly with frequency, which is in agreement with other

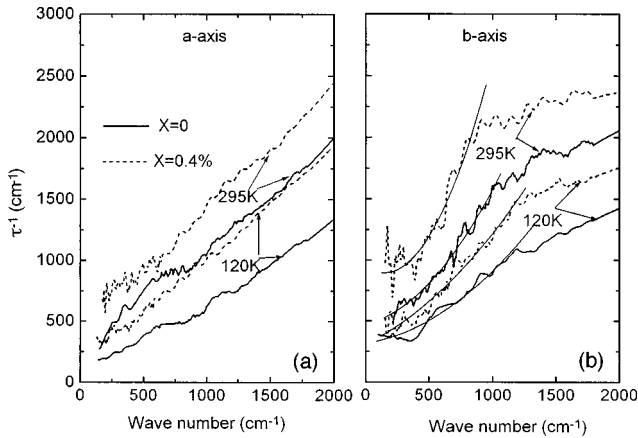


FIG. 3. Frequency-dependent scattering rates for two samples in the  $a$  axis (a) and  $b$  axis (b). The thin solid curves in (b) are fits to the  $\omega^2$  dependence.

reports,<sup>9</sup> while the  $b$ -axis scattering rate shows approximately the  $\omega$ -square dependence in the far-infrared region, then reduces the rate to a  $\omega$ -linear dependence. This  $\omega$ -square dependence of scattering rate should be related to the  $T$ -square dependence of the dc resistivity in the  $b$  direction.<sup>12</sup> The overall plasma frequency is defined in terms of the sum rule  $\omega_p^2/8 = \int_0^{\omega_{\max}} \sigma_1(\omega) d\omega$  with  $\omega_{\max} = 10\,000 \text{ cm}^{-1}$ . We obtained  $\omega_{pa} = 1.95 \times 10^4 \text{ cm}^{-1}$ ,  $\omega_{pb} = 2.62 \times 10^4 \text{ cm}^{-1}$  for the pure sample, and  $\omega_{pa} = 1.94 \times 10^4 \text{ cm}^{-1}$ ,  $\omega_{pb} = 2.42 \times 10^4 \text{ cm}^{-1}$  for the 0.4% Zn-substituted sample.<sup>13</sup> There is almost no change in  $\omega_{pa}$  upon Zn substitution, while  $\omega_{pb}$  shows some decrease. As a result, the in-plane anisotropy is slightly reduced.

A more striking Zn-substitution effect is observed in the superconducting state. Below  $T_c$ , a substantial amount of spectral weight has been missed in  $\sigma_1(\omega)$ , which should appear in the zero-frequency  $\delta$  function. When Zn is substituted, a very pronounced Drude-like response is observed at low frequency. This is due to the remaining unpaired carriers which fill up the states in the gap. As a result, the missing areas are significantly reduced in all three directions in the Zn-doped samples. The London penetration depth can be calculated from the missing areas as  $\lambda^{-2} = \omega_{ps}^2/c^2 = (8/c^2) \int_0^{\omega_{ps}} (\sigma_{1n} - \sigma_{1s}) d\omega$ , where  $\omega_{ps}$  is the superfluid plasma frequency,  $c$  the speed of light, and  $\sigma_{1n}$  and  $\sigma_{1s}$  the conductivity in the normal and superconducting states. The superfluid plasma frequency is related to the superfluid density  $n_s$  through  $\omega_{ps} = (4\pi n_s e^2/m^*)^{1/2}$ , where  $m^*$  is the effective mass. The obtained penetration depths at 8 K are  $\lambda_a = 1600 \text{ \AA}$ ,  $\lambda_b = 1170 \text{ \AA}$ , and  $\lambda_c = 12\,000 \text{ \AA}$  for the pure sample,  $\lambda_a = 3400 \text{ \AA}$ ,  $\lambda_b = 3300 \text{ \AA}$  for the sample with Zn concentration  $x = 0.4\%$ , and  $\lambda_c = 20\,600 \text{ \AA}$  for  $x = 0.6\%$ . The  $c$ -axis penetration depth for another sample with higher Zn content  $x = 1.3\%$  is estimated to be  $28\,300 \text{ \AA}$ . The values obtained for the pure sample with  $\mathbf{E} \parallel a$  and  $\mathbf{E} \parallel b$  are in good agreement with the reported data.<sup>10</sup> In Fig. 4, we plot the inverse square of the penetration depth relative to that of the pure sample as a function of relative decrease in  $T_c$ . The dashed curve is the theoretical calculation for a  $d$ -wave-pairing symmetry and nonmagnetic elastic scattering in the unitary limit.<sup>14,4</sup> Note that our data are not in agreement with the conventional theoretical calculation for a

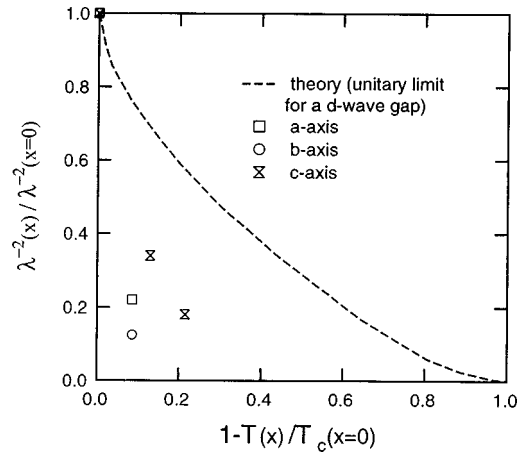


FIG. 4. Plot of the normalized inverse square of the penetration depth as a function of the relative decrease in  $T_c$ .

$d$ -wave-pairing symmetry in two aspects. First, the suppression of the condensate is much stronger than the theoretical calculation. Second, the suppression is anisotropic. The condensate density is most strongly suppressed in the  $b$  direction, but least in the  $c$  direction.

Dramatic suppression of the condensate is the most notable result in this work. The suppression of the transition temperature is less than 10% by 0.4% Zn substitution, whereas the suppression of the condensate density reaches 78% in the  $a$  direction. The data are in strong contrast to the  $\mu$ SR study by Nachumi *et al.*<sup>15</sup> on polycrystalline samples, showing that the Zn substitution falls into the same correlation of  $T_c$  with  $n_s/m^*$  found for a variety of cuprate superconductors.<sup>16</sup> The present result requires an additional mechanism to explain such an extremely strong pair-breaking effect. We speculate that magnetic scattering should be taken into account since the NMR measurements reveal that Zn induces a local magnetic moment on neighboring Cu sites.<sup>17,18</sup> With regard to the suppression of anisotropy within the  $ab$  plane, there are two possible interpretations. One is based on the single band model with a  $(d+s)$ -wave-pairing symmetry. It is predicted that the zero temperature penetration depth is more affected in the  $b$  direction than in the  $a$  direction by impurities in the case of  $(d+s)$ -wave symmetry.<sup>19</sup> Within such a one-band model, this experimental result suggests that Zn impurities suppress the  $s$ -wave component in the pairing symmetry, because the in-plane anisotropy in the penetration depth is actually reduced. Another possibility for the anisotropy suppression is based on the two-band model, in which it is assumed that the CuO chains in YBCO form an independent conduction band and contribute to the superconducting condensate.<sup>20,21</sup> In this scenario, the experimental result implies that Zn substitution not only suppresses the condensate in the plane but also destroys the additional condensate in the chains.

Concerning the  $c$ -axis suppression, no concrete theory is currently available to be compared with. We note that the ac susceptibility measurement also suggests that the penetration depth along the  $c$  axis is less affected than that within the  $ab$  plane.<sup>22</sup> Our optical data are consistent with this measurement.

In summary, we have presented the polarized optical measurement on Zn-doped YBCO. We showed that Zn seriously

affects the low-energy charge dynamics in both normal and superconducting states. Zn substitution increases the scattering rates, which leads to the reduction of dc conductivities in all three directions in the normal state. In addition, Zn reduces the in-plane anisotropy by suppressing the plasma frequency in the  $b$  direction. In the superconducting state, we

observe very strong and anisotropic suppression of the superfluid density along three crystallographic axes, which cannot be accounted for by the nonmagnetic impurity scattering for a pure  $d$ -wave superconductor.

We thank W. A. Atkinson for helpful discussions. This work was partially supported by NEDO.

- 
- <sup>1</sup>K. Ishida *et al.*, J. Phys. Soc. Jpn. **62**, 2803 (1993).  
<sup>2</sup>J. W. Loram *et al.*, Physica C **235-240**, 134 (1994).  
<sup>3</sup>D. A. Bonn *et al.*, Phys. Rev. B **50**, 4051 (1994).  
<sup>4</sup>C. Bernhard *et al.*, Phys. Rev. Lett. **77**, 2304 (1996).  
<sup>5</sup>A. I. Rykov *et al.*, in *Advances in Superconductivity VIII*, edited by H. Hayakawa and Y. Enomoto (Springer-Verlag, Tokyo, 1996).  
<sup>6</sup>S. Tajima *et al.*, J. Opt. Soc. Am. B **6**, 475 (1989).  
<sup>7</sup>S. L. Cooper *et al.*, Phys. Rev. B **47**, 8233 (1993).  
<sup>8</sup>T. Timusk *et al.*, J. Supercond. **8**, 437 (1995).  
<sup>9</sup>Z. Schlesinger *et al.*, Phys. Rev. Lett. **65**, 801 (1990).  
<sup>10</sup>D. N. Basov *et al.*, Phys. Rev. Lett. **74**, 598 (1995).  
<sup>11</sup>T. Timusk and D. B. Tanner, in *Physical Properties of High Temperature Superconductors*, edited by D. M. Ginsberg (World Scientific, Singapore, 1992), Vol. III, p. 339.  
<sup>12</sup>R. Gagnon *et al.*, Phys. Rev. B **50**, 3458 (1994).  
<sup>13</sup>We note that the values of  $\omega_p$  obtained here are somewhat ambiguous because of the arbitrarily chosen cutoff frequency for the upward limit of the integration. However, for comparison, the same cutoff frequency was used.  
<sup>14</sup>Y. Sun and K. Maki, Phys. Rev. B **51**, 6059 (1995).  
<sup>15</sup>B. Nachumi *et al.*, Phys. Rev. Lett. **77**, 5421 (1996).  
<sup>16</sup>Y. J. Uemura *et al.*, Phys. Rev. Lett. **62**, 2317 (1989).  
<sup>17</sup>H. Alloul *et al.*, Phys. Rev. Lett. **67**, 3140 (1991).  
<sup>18</sup>S. Zagoulaev *et al.*, Phys. Rev. B **52**, 10 474 (1995).  
<sup>19</sup>Heesang Kim and E. J. Nicol, Phys. Rev. B **52**, 13 576 (1995).  
<sup>20</sup>W. A. Atkinson and J. P. Carbotte, Phys. Rev. B **52**, 10 601 (1995); **55**, 14 592 (1997).  
<sup>21</sup>T. Xiang and J. M. Wheatley, Phys. Rev. Lett. **76**, 134 (1995).  
<sup>22</sup>C. Panagopoulos *et al.*, Phys. Rev. B **54**, R12 721 (1996).